Construction and Building Materials 124 (2016) 746–754

Contents lists available at ScienceDirect

Construction and Building Materials

journal homepage: www.elsevier.com/locate/conbuildmat

Effect of strain rate on post-peak cyclic behavior of concrete in direct tension

Xudong Chen [a,*], Jingwu Bu [b], Lingyu Xu [a]

[a] College of Civil and Transportation Engineering, Hohai University, Nanjing 210098, PR China
[b] College of Water Conservancy and Hydropower Engineering, Hohai University, Nanjing 210098, PR China

HIGHLIGHTS

- Post-peak cyclic behavior of concrete in direct tension is studied.
- Various loading regimes are performed on concrete in tension.
- Strain rate effect on the post-peak stress-strain response is considered.
- Stress releases and damage accumulations are independent of strain rate.
- Damage constitutive model is proposed to describe the stress-strain relation.

ARTICLE INFO

Article history:
Received 8 May 2016
Received in revised form 15 June 2016
Accepted 4 August 2016
Available online 8 August 2016

Keywords:
Cyclic
Direct tension
Post-peak
Constitutive model
Damage accumulation

ABSTRACT

A test method has been developed to obtain reliable post-peak cyclic behavior of concrete in this study. Considering three various loading regimes, strain rate effect on post-peak stress-strain response of concrete is investigated. The envelope curve is found coincides with the monotonic loading curve, which is shown to govern the cyclic response. Concrete presents slightly rate sensitive when it is subjected to static loading. The tensile strength increases with the increasing of strain rate. The stress releases with cyclic even if the maximum strain is constant. It demonstrated that the stress release process is independent of strain rate and it can be expressed by a power function. Analytical expressions introducing damage index are proposed to describe the entire monotonic behavior, as well the response to cyclic loadings. The analytical model uses the concept of uniqueness of envelope curve. The calculated results predicted by the analytical expressions have good agreement with test data.

1. Introduction

It is well known that concrete exhibits post-peak softening behavior, in which large strains are involved. To investigate the softening behavior of concrete the complete stress strain curve need to measure. The development of testing machine and computer technique in recent years has promoted the investigation on cyclic behavior of concrete. The first work considering the cyclic behavior of concrete was published by Sinha et al. [1], in which a significant concept of uniqueness of envelope curve was put forward. Subsequently, numerous constitutive models have been proposed in the last few decades. Sima et al. [2] proposed a constitutive model for concrete subjected to cyclic loadings in compression and tension, in which two independent damage variables in compression and in tension have been introduced. To improve the damage accumulation evolution, Breccolotti et al. [3] modified the model proposed by Sima et al. This model took into account the damage increment in concrete under constant and variable amplitude loadings.

Except the damage constitutive models, thermodynamic models have also been developed. Lee and Fenves [4] proposed a plastic damage model based on continuum damage mechanics. This model used two damage variables for concrete in tension and compression. To better and truly describe the plasticity and damage of plain concrete, Cicekli et al. [5] introduced an anisotropic damage with new plasticity yield and damage criteria in the plastic-damage constitutive mode. Tensile and compressive damage criteria are separately used in the model, which took also into account the stiffness recovery caused by crack opening and closing.

These above models have been evaluated by simulating experimental stress strain curves of plain concrete and reinforced concrete subjected to cyclic compression. However, only a few

* Corresponding author.
E-mail addresses: cxdong1985@hotmail.com (X. Chen), bujingwu2008@163.com (J. Bu), xulingyu1994@126.com (L. Xu).

http://dx.doi.org/10.1016/j.conbuildmat.2016.08.012
0950-0618/

models consider the tension response because direct tension test on concrete is difficult to conduct. In recent years, Chen et al. [6–8] have performed experimental researches on dynamic tensile behavior of concrete. Ranaivomanana et al. [9] and Alhussainy et al. [10] have studied the creep behavior of normal concrete in tension and stress-strain relation of self-compacting concrete by improving the direct tensile test method, respectively. However, the cyclic tensile behavior has ever been concerned little [11–14]. Xiao et al. [11] studied the fatigue strain variation and the fatigue modulus degradation of recycled aggregate concrete. Yankelevsky and Reinhardt [12] proposed analytical expressions describing both the entire monotonic and cyclic response of concrete. Rather simple expressions have been proposed to reproduce any unloading or reloading curve as function of the starting point coordinates. Reinhardt and Cornelissen [13] established complete stress-deformation curves for concrete in tension and alternating tension-compression. Crack growth and strain distribution around the crack tip of concrete in cyclic tension was studied. Gopalaratnam and Shah [14] developed an available testing method to obtain reliable complete load-deformation curve in direct tension. They performed both monotonic and cyclic tests and developed an analytical expression to describe the entire tensile response of concrete. However, the analytical expression is not applicable to cyclic stress strain response. Some simple constitutive models have been proposed and evaluated by using experimental results from the above literatures [2,15–17]. Constitutive formulations are presented for concrete subjected to reverse cyclic loading consistent with a compression field approach by Palermo and Vecchio [15]. Features of the modeling include: nonlinear unloading using a ramberg-osgood formulation; linear reloading that incorporates degradation in the reloading stiffness based on the amount of strain recovered during the unloading phase; and improved plastic offset formulations. Formulations for partial unloading and partial reloading are also presented. Additionally, the authors used a straight line to model the unloading and reloading branches in tension under cyclic loading when there is no incursion in compression during a cycle. This concept is used by Forster and Mati [16], Mansor and Hsu [17], and Sima et al. [2].

Non-elastic materials like concrete have strain rate sensitive characteristic which have been verified by numerous researches [6,7,18]. It was demonstrated that the strength increases with increasing of strain rate by performing dynamic mechanical tests on concrete. However, the effect of strain rate on the post-peak cyclic behavior is not concerned.

Experimental results about stress strain response of concrete subjected to cyclic tension are still limited. The existing models are always based on their own experimental results, which need further verification by other test results. So the existing constitutive models are not verified capable to arbitrary loading conditions. In this paper, an experimental study on the constitutive behavior of concrete subjected to cyclic tension is carried out. To obtain a complete understanding of cyclic post-peak behavior of concrete in tension, tests are performed on concrete specimens at various loading regimes. The effects of strain rate on the cyclic post-peak behavior are also performed in this study. Analytical expressions introducing damage index is proposed to describe the entire monotonic behavior, as well the response to cyclic loadings. Finally, comparisons with typical test data are shown in this paper.

2. Experimental program

2.1. Test specimens

During the present study tests have been performed on specimens made of the same concrete mix proportions (shown in Table 1) and having a same geometry: cylinder specimens with diameter of 73 mm and height of 146 mm. The concrete is a mixture of ordinary Portland cement and secondary fly ash, river sand with particle size distribution fitting ASTM C33 [19], aggregates of 20 mm maximum size, portable water and polycarboxylate superplasticizer to obtain a well flow-ability. The concrete was cast into cylinder PVC pipes in diameter of 73 mm and kept in curing room for one day. After demolding the specimens were cured under water for 7 days, and then cured in nature till 28 days. Before testing the concrete cylinders were cut in height of 146 mm. The two ends of cylinder specimen were paste into the steel platen by structural adhesive to get enough adhesive strength before testing. The instrumented cylinder concrete is shown in Fig. 1.

Table 1
Concrete mix proportions by weight.

Mass of concrete ingredients (kg/m^3)					
Water	Cement	Fly ash	Sand	Aggregate	Water Reducer
205	328	82	668	1089	2.05

2.2. Loading and measurement

The tests were carried out on a servo controlled electro-hydraulic material testing system (MTS 322) equipped with two manufactured spherical joints to reduce eccentricity in testing. The load transferred to the specimen by the spherical joints and screws. Across the lateral three LVDTs (linear variable differential transducer) were attached to the concrete with a measuring length of 140 mm under 120° between each other. The three strain values were recorded. And the strain values were averaged and fed into a variable-gain amplifier, so a specific strain rate was achieved. Three different strain rates of 1 με/s, 5 με/s and 10 με/s were performed on specimens in this study.

Fig. 1. Instrumented concrete cylinder.

Table 2
Test specimens and the corresponding loading procedure.

Test specimen	$\dot{\varepsilon}$	Loading procedure
CEN1-1	1 με/s	Cycles to envelope curve
CEN2-5	5 με/s	Cycles to envelope curve
CEN3-10	10 με/s	Cycles to envelope curve
CSI50-1	1 με/s	Cycles with constant strain increment of 50 με
CSI30-5	5 με/s	Cycles with constant strain increment of 30 με
CSI60-10	10 με/s	Cycles with constant strain increment of 60 με
CMS120-1, CMS130-1	1 με/s	Cycles with constant maximum strain amplitude of 120/130 με
CMS100-5, CMS120-5	5 με/s	Cycles with constant maximum strain amplitude of 100/120 με
CMS120-10, CMS230-10	10 με/s	Cycles with constant maximum strain amplitude of 120/230 με

To investigate completely the post peak softening response of concrete, three loading regimes are employed summarized as Table 2. Besides, the monotonic tension tests are also carried out to compare with the envelope curve for same batch specimens. For monotonic loading, 3 specimens are performed for each strain rate. For cyclic loading, one specimen is tested for each loading history in terms of loading regime and strain rate.

3. Envelope curve

3.1. Experimental results

Specimens fractured at a random location along the axial direction of specimen, the failure mode and fracture pattern as shown in Fig. 2.

A generally accepted concept in the literature about concrete subjected to cyclic loading is that there is a unique envelope curve coincides with or similar to the monotonic curve. Most authors have confirmed the concept by performing tests on mortar [20], plain concrete [1,21], and reinforced concrete [22]. As illustrated in Fig. 3, this concept also applies to plain concrete subjected to cyclic tension in regard to various loading history.

3.2. Concept of damage model

The objective of this section is to develop analytical expressions incorporating the damage index for response of concrete. The analytical model is based on the following assumptions [3]: (1) the damage function is a non-decreasing function; (2) there is no damage increase in the unloading branches since no external work acted on it; (3) an univocal correspondence exists between the envelope curve points and the residual strain; (4) the damage accumulates in the reloading curve is not linear. The damage increases slightly up to the proximity of the envelope curve where it begins to grow faster.

A linear expression represents well the pre-peak branch of concrete in tension and many researchers [2,23] have used this method. The post-peak branch shows highly nonlinear softening behavior, so it is difficult to describe it by simple mathematical functions. So far, polylinear expression [24], exponential expression [14] or combined expressions [12] have been employed to fitting the softening branch. In the present study, piecewise expressions including a linear relation until reaching the tensile strength and a combined mathematical expression were proposed to formulate the response of concrete subjected to monotonic tensile loading.

As the pre-peak branch can be assumed as elasticity, the stress strain curve of concrete in tension can be expressed as a simple linear equation as follow:

$$\sigma = \varepsilon E_0, \text{for} \quad \varepsilon \leqslant \varepsilon_t \tag{1}$$

where, σ is tensile stress, ε is tensile strain, $E_0 = f_t/\varepsilon_t, f_t$ is the tensile strength, ε_t is the strain corresponding to the tensile strength. The pre-peak branch can be obtained by using the characteristic value of f_t and ε_t.

A combined mathematical formulation to describe the post-peak behavior is developed by fitting with the experimental results as follow:

$$\sigma = f_t\left\{a - b\frac{\varepsilon}{\varepsilon_t} + c\exp\left[\mathrm{d}\left(1 - \frac{\varepsilon}{\varepsilon_t}\right)\right]\right\}, \text{for } \varepsilon \geqslant \varepsilon_t \tag{2}$$

where, a, b, c, d are constants which have been obtained by fitting the post-peak branch for different strain rates. $a = 0.23$, $b = 0.03$, $c = 0.80$ and the value of them are independent of strain rate.

Fig. 2. The fracture pattern of concrete specimens under direct tensile loading.

Parameter d is equal to 1.56, 1.80, and 1.92 for strain rates of 1 με/s, 5 με/s and 10 με/s respectively. The variance of parameter d presents the effect of strain rate on curvature of post-peak branch, which implies that the post-peak behavior of concrete have strain rate sensitive.

Assuming that stress σ can be formulated by a function of strain and damage variable δ:

$$\sigma = (1-\delta)E_0\varepsilon \tag{3}$$

As the pre-peak is assumed to be linear elastic with no damage accumulation, so the damage index is deemed as 0. For the post-peak branch the damage index δ turns out to have the following definition:

$$\delta = 1 - \frac{\sigma}{E_0\varepsilon} = 1 - \left\{a - b\frac{\varepsilon}{\varepsilon_t} + c\exp\left[d\left(1-\frac{\varepsilon}{\varepsilon_t}\right)\right]\right\}\frac{\varepsilon_t}{\varepsilon} \tag{4}$$

Based on the above assumption and the damage concept of concrete, the damage evolution is plotted with the corresponding stress strain curve in Fig. 4.

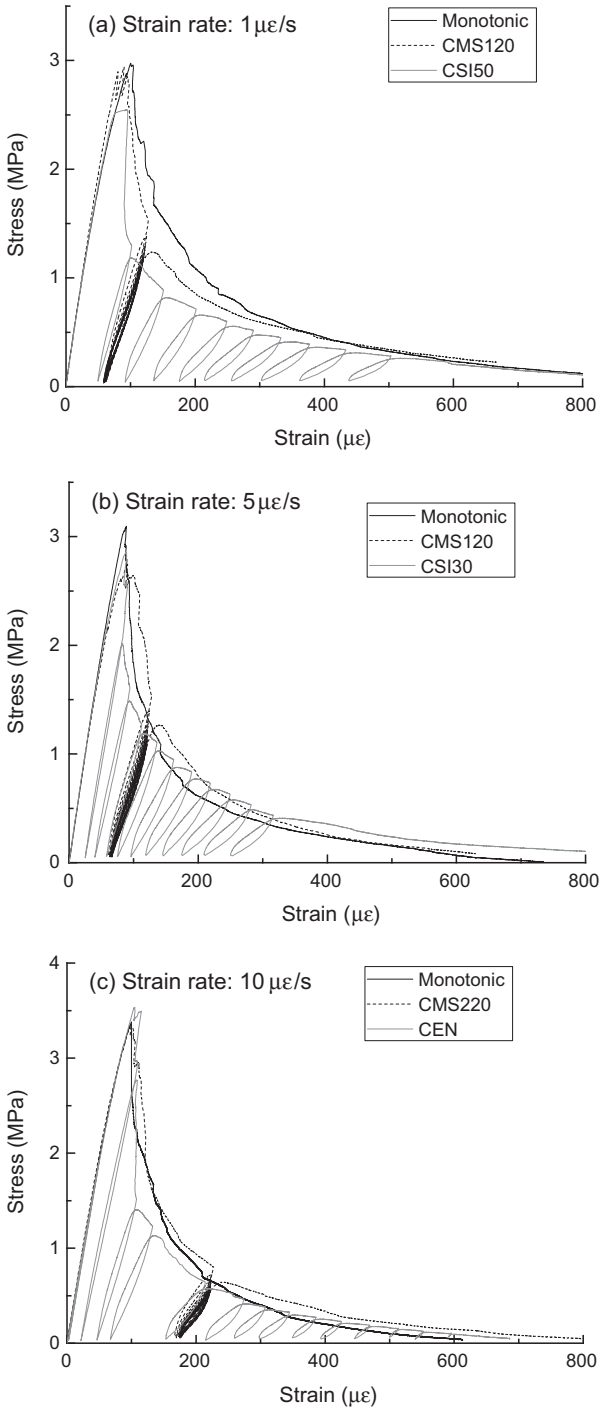

Fig. 3. Typical stress strain response of concrete subjected to cyclic and monotonic loading at various strain rates: (a) 1 με/s, (b) 5 με/s, (c) 10 με/s.

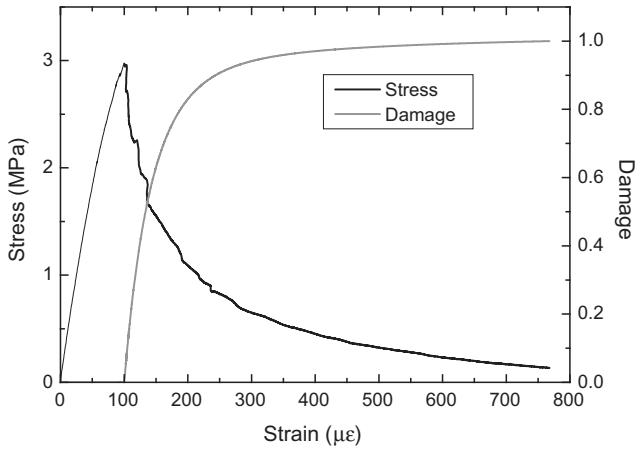

Fig. 4. Damage evolution and the corresponding stress-strain curve.

3.3. Comparison with experimental results

The proposed model has been evaluated by comparing the analytical results with experimental data as shown in Fig. 5. It is observed that a linear expression is adequate for the pre-peak branch. The nonlinear post-peak branch is simulated by the combined mathematical expression. The envelope curve is also predicted by the proposed model only demanding for the tensile strength f_t and the corresponding strain ε_t.

4. Stress strain response of concrete in cyclic tension

When a concrete is tested by strain controlled method in tension, it first reacts elastically. A linear stress-strain relation almost up to peak stress can be obtained. When it reaches to peak stress of concrete, the strain of concrete starts to localize within a narrow zone of micro-cracks, after which a continuous macro-crack will

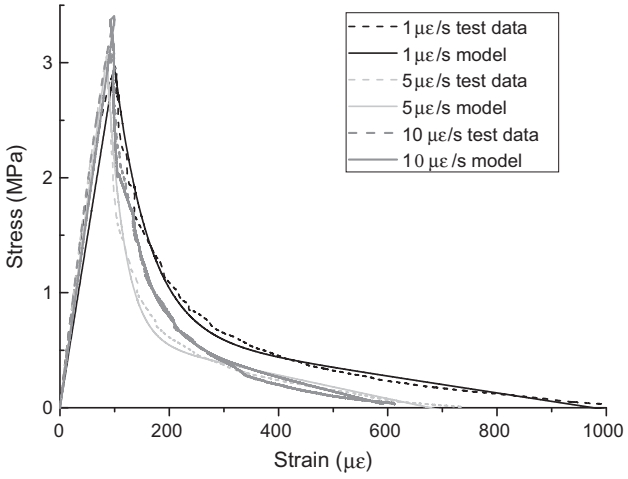

Fig. 5. Comparison of predicted results with the experimental results for concrete in monotonic tension.

develop. The micro-cracks will occur at the weakest section of concrete in tension. The softening branch will be obtained if the micro-cracks develop within the measuring length whose deformation is used as the control parameter. According to the fictitious crack model by Hillerberg and co-workers, the deformation in the descending branch is built up by strains and crack opening. In this paper, the authors attend to develop a macro-level constitutive model to describe the post-peak stress-strain relationship of concrete in cyclic tension, so only the average strain and stress were considered rather than crack opening.

4.1. Residual strain

Residual strain is defined as the strain corresponding to a near-zero stress level on the unloading stress strain path. The residual strain increases with the increasing of envelope unloading strain where unloading starts. The increase of envelope unloading strain ε_{eu} causes approximately the same increase of residual strain ε_r as shown in Fig. 6. As illustrated in Fig. 6 that the accumulation rates of residual strain is slightly different for various strain rates. Linear mathematical expressions are formulated as Eqs. (5)–(7) in order to quantify the effect of strain rate on residual strain accumulation. The slope of the linear expression for strain rate of 1 με/s is smaller than 1 which implies the accumulation rate of residual strain is slower than that of envelope unloading strain. At the strain rates of 5 με/s and 10 με/s the slope for ε_r versus ε_{eu} is larger than 1, which means that the accumulation rate of residual strain is faster than that of the envelope unloading strain. The slopes for ε_r versus ε_{eu} for various strain rates show that the higher the strain rate is, the faster the accumulation rate of residual strain.

$$\varepsilon_r = 0.98\varepsilon_{eu} - 53.70 \text{ for } \dot{\varepsilon} = 1\ \mu\varepsilon/s \tag{5}$$

$$\varepsilon_r = 1.06\varepsilon_{eu} - 65.32 \text{ for } \dot{\varepsilon} = 5\ \mu\varepsilon/s \tag{6}$$

$$\varepsilon_r = 1.13\varepsilon_{eu} - 85.85 \text{ for } \dot{\varepsilon} = 10\ \mu\varepsilon/s \tag{7}$$

4.2. Stress release

Stress release is observed even if the maximum strain is constant, when the specimen is subjected to cyclic to constant maximum strain. Fig. 7 shows the stress release versus the number of cycles for cyclic to constant maximum strain for specimens. Fig. 7 shows that the rate of stress release decreases with the cycling continues. Rapid stress release can be observed for the first few cycles and then keep stability for all range of specified maximum strain. The stress release versus loading cycles can be universally expressed as Eq. (8).

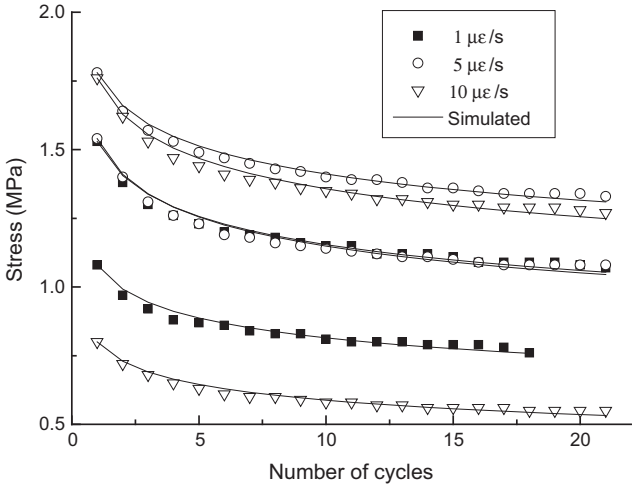

Fig. 7. Stress release versus number of cycles for cyclic to constant strain amplitude.

$$\sigma = \sigma_{\max} N^t \tag{8}$$

where, σ is the stress corresponding to Nth cycle to the same maximum strain, and $\sigma_{\max}$ corresponds to the first cycle, N is the number of cycle to the same maximum strain. t is an empirical parameter equal to −0.12. The simulated result is compared with experimental results as shown in Fig. 7.

These experimental results indicate that the specimen present apparent stabilization in the stress which means damage accumulation has been stabilized.

4.3. Damage for the reloading strain

When a complete unloading and reloading up to the envelop curve are performed on the specimen, the damage variable can be assumed as follow by fitting the experimental results:

$$\delta_{er} = 1.075\delta_{eu} - 0.075\delta_{eu}^2 \tag{9}$$

where, δ_{er} is the damage for envelope reloading, and δ_{eu} is the damage for envelope unloading. The relationship of damage for envelope reloading versus the damage for envelope unloading shown in Fig. 8 is a polynomial function rather than a linear function. This function allows specific damage accumulation under small stress

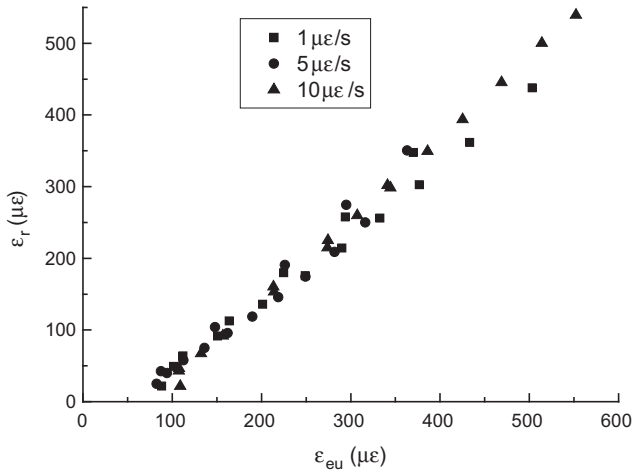

Fig. 6. Relation of residual strain versus the envelope unloading strain.

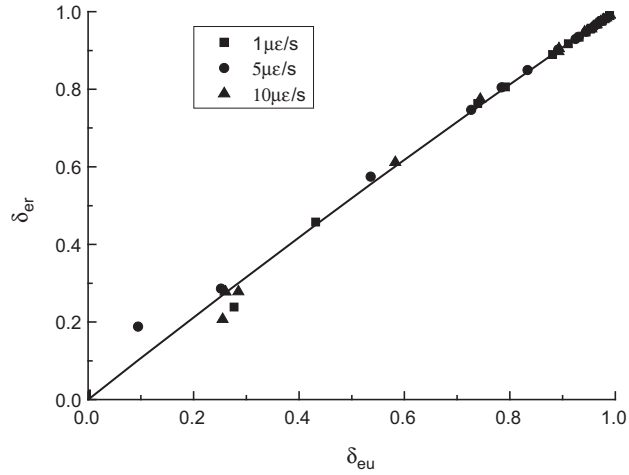

Fig. 8. The relationship of δ_{er} versus δ_{eu}.

cycles performed on the undamaged material. This fitting curve through the points with coordinates $(\delta_{eu}, \delta_{er})$ is equal to (0, 0) and (1, 1) to avoid the damage index is greater than 1 for values of δ_{eu} is approximated to 1.

Berccolotti et al. [3] assumed that the damage accumulated slowly at the beginning of the reload path while faster damage accumulation is foreseen for higher stress level. In the present paper, the same concept is used to study the damage accumulation in reload path, which can be expressed as follows:

$$\delta = \delta_r + (\delta_{er} - \delta_r)\left(\frac{\sigma}{\sigma_{er}}\right)^6 \tag{10}$$

where, δ_r is the damage corresponding to the residual strain and it is assumed to be equal to the damage δ_{eu} since no external energy applied to the system when unloading.

4.4. Model for complete unloading and reloading path

The experimental results show that unloading curve is convex to the right for an entire strain range, while the reloading curve is convex to the left for all strain range. The shape of unloading and reloading curve shows stability for an entire strain range. So power type function can be selected as its stability to model the unloading and reloading curve rather than the polynomial or exponential type. The mathematical expression in power type can reflect the nonlinearity (i.e. the damage) of concrete. The schematic of unloading branch is shown in Fig. 9(a).

The unloading stress-strain relationship can be expressed as

$$\sigma = \sigma_r + c_u(\sigma_{eu} - \sigma_r)\left(\frac{\varepsilon - \varepsilon_r}{\varepsilon_{eu} - \varepsilon_r}\right)^{p_u} \tag{11}$$

in which, σ and ε are the stress and strain along the unloading path, σ_r and ε_r are the stress and strain corresponding to the end point of unloading path. In the case of complete unloading, the coordinates $(\varepsilon_r, \sigma_r)$ is equal to $(\varepsilon_r, 0)$, σ_{eu} and ε_{eu} are the envelope unloading stress and strain. The parameters, c_u and p_u can be determined by fitting the experimental data. The fitting results show that the coefficient c_u is approximate to 0.95 for all unloading strain. Based on the behavior of unloading in the present tests and the above mentioned preliminary shape of unloading curve, p_u is found to be greater than 1. The value of p_u increases with the increasing of damage accumulation. The power p_u can be expressed as a function of damage index and the strain rate since the curvature and shape of unloading curve is dependent on the load history.

$$p_u = 1 + \delta_{eu}^t \tag{12}$$

with

$$t = 5.59 + 7.37\dot{\varepsilon}\exp[\log(\dot{\varepsilon}) + 15.33] \tag{13}$$

where, δ_{eu} is the damage index corresponding to the envelope unloading strain, $\dot{\varepsilon}$ is the strain rate.

The reloading branch can be expressed similar to the unloading branch as follow:

$$\sigma = \sigma_r + c_r(\sigma_{er} - \sigma_r)\left(\frac{\varepsilon - \varepsilon_r}{\varepsilon_{er} - \varepsilon_r}\right)^{p_r} \tag{14}$$

where, c_r is the reloading coefficient close to 1 and p_r is the power which can be expressed as a function of the damage parameter corresponding to envelope reloading strain and is independent of the strain rate.

$$p_r = 1 - 0.52\delta_{er}^{0.44} \tag{15}$$

where, δ_{er} is the damage corresponding to the envelope reloading strain.

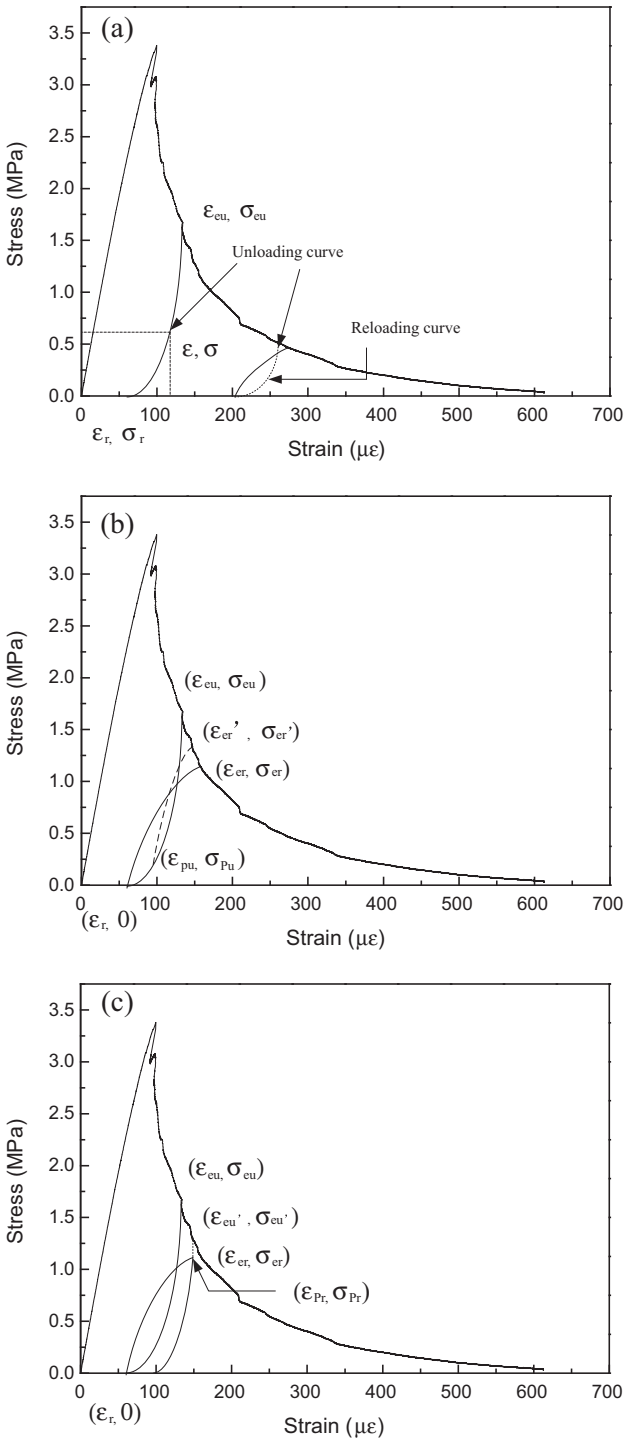

Fig. 9. (a) Cycle with complete unloading and reloading path, (b) Cycle with complete reloading after incomplete unloading, (c) Cycle with complete unloading after incomplete reloading.

4.5. Model for reload after incomplete unload

In the case of an incomplete unloading seen in Fig. 9(b) the stress strain path interrupts the unloading branch at the point $(\varepsilon_{pu}, \sigma_{pu})$. Since there is no damage accumulates in the unloading path, it satisfies the equation $\delta_{pu} = \delta_{eu}$. The corresponding stress can be calculated by Eq. (11). The shape of reloading curve after incomplete unloading is assumed to be linear, it is directed towards the point $(\varepsilon'_{er}, \sigma'_{er})$ on the envelope curve. If the unloading

is incomplete the damage accumulation is not complete after reloading to the envelope curve compared to the reload after complete unloading. So the point $(\varepsilon'_{er}, \sigma'_{er})$ can be located between $(\varepsilon_{eu}, \sigma_{eu})$ and $(\varepsilon_{er}, \sigma_{er})$ and the corresponding damage δ'_{er} should be smaller than δ_{er} but greater than δ_{pu}. In order to determine the point $(\varepsilon'_{er}, \sigma'_{er})$, the following procedure is performed: (1) give a series strain values $\varepsilon_1, \varepsilon_2, \ldots \varepsilon_n$ with small enough intervals between ε_{eu} and ε_{er} and compute the corresponding damages $\delta_1, \delta_2, \ldots \delta_n$ by using Eq. (4). (2) Compute a series damage values $\delta_{r1}, \delta_{r2}, \ldots \delta_{rn}$ near zero stress point $(\varepsilon_r, 0)$ seen in Fig. 8(b) corresponding to the assumed series strain values. In the series damage values $\delta_{r1}, \delta_{r2}, \ldots \delta_{rn}$ among which a damage value δ_{ri} is equal to δ_{pu}. The damage δ'_{er} at the envelope reloading point can be determined according to the damage δ_{ri} by using Eq. (8). The corresponding reloading strain ε'_{er} can be calculated from δ'_{er} according to Eq. (4). As long as the reloading strain ε'_{er} is given, the reloading path can be predicted by using Eq. (14).

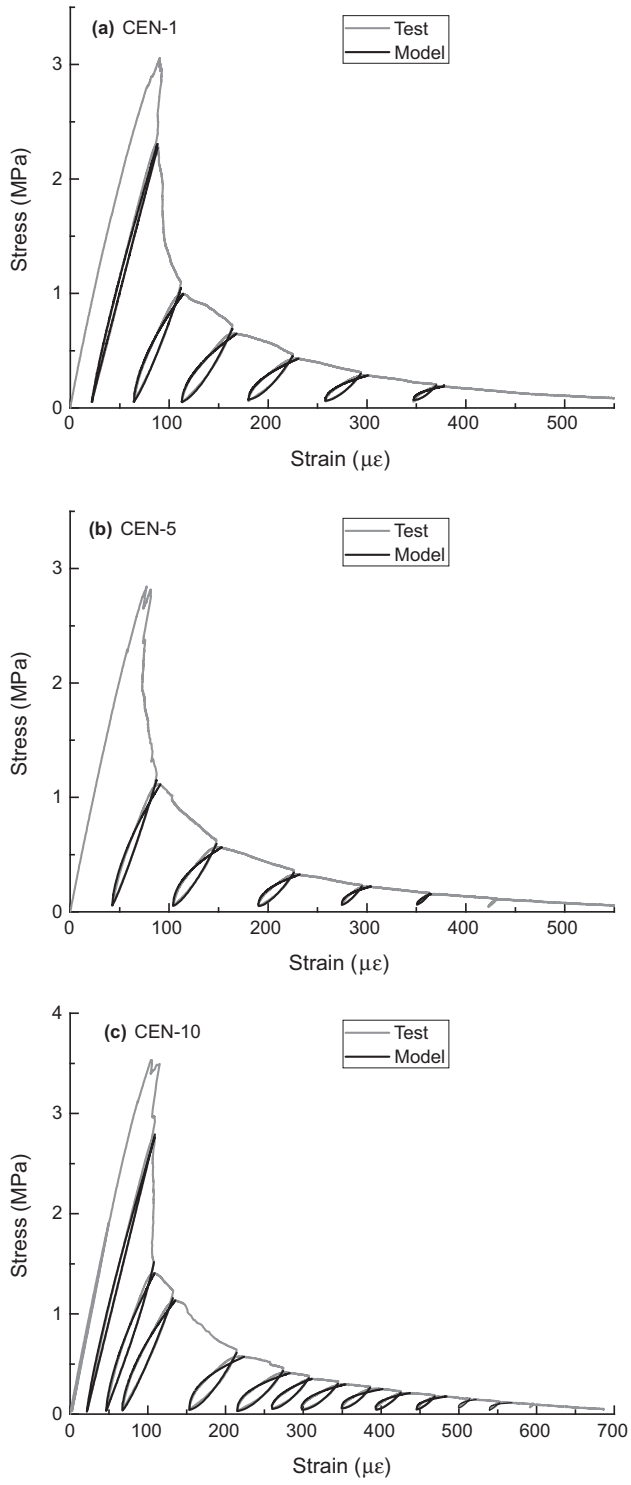

Fig. 10. Comparison of predicted results with experimental tests from cyclic to envelope curve at various strain rates.

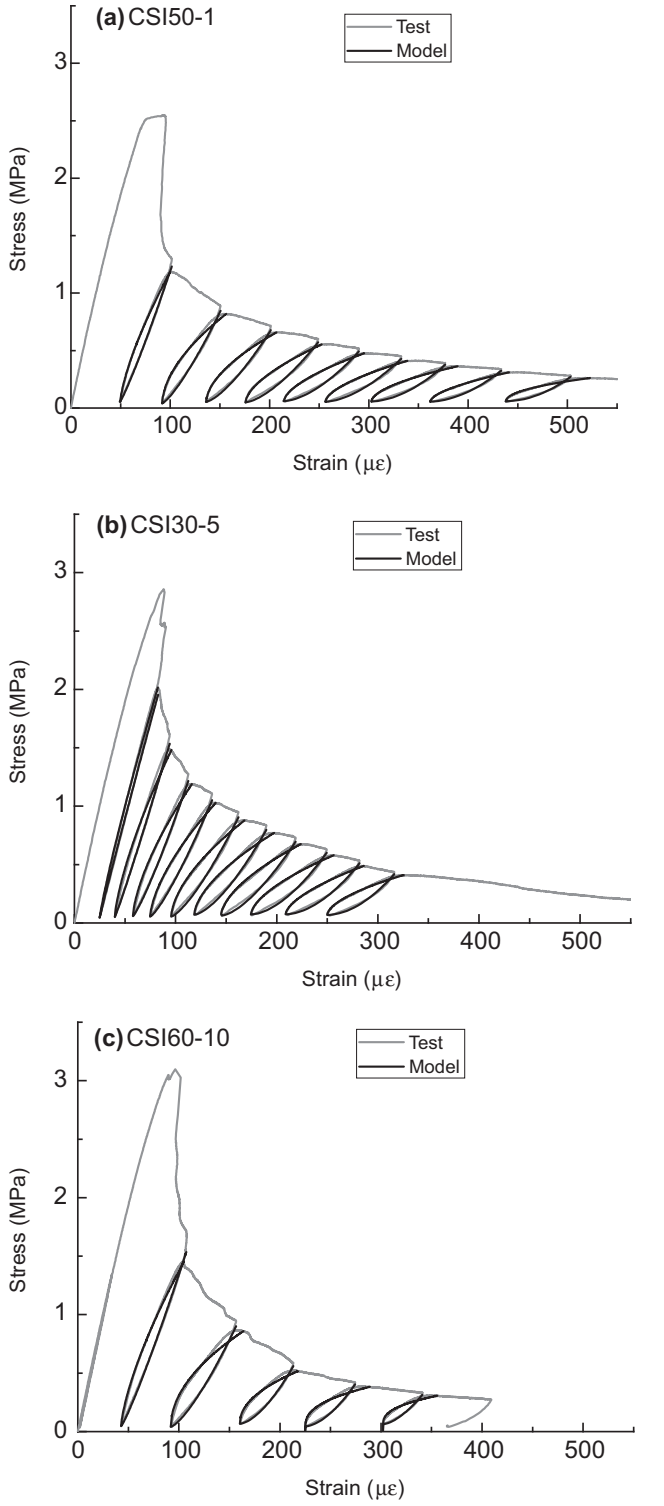

Fig. 11. Comparison of predicted results with experimental tests from cyclic with constant increment strain at various strain rates.

4.6. Model for unloading after an incomplete reloading

In the case of an incomplete reloading, the stress strain path interrupts at the point $(\varepsilon_{pr}, \sigma_{pr})$ (seen in Fig. 9(c)) and the corresponding damage δ_{pr} can be calculated by Eq. (9). Along the envelope curve, there is a point which possesses the same damage as that at the end point of reloading, and the corresponding strain can be calculated by inverting Eq. (4). Since no damage accumulation along the unloading path, unloading path from the end point of incomplete reloading $(\varepsilon_{pr}, \sigma_{pr})$ and from the point on the envelope curve possesses the same damage have a same residual strain. The residual strain can be computed by Eqs. (5)–(7). As long as the residual strain has been determined, the unloading branch after an incomplete reloading can be described by Eq. (11).

4.7. Comparison with experimental results

Predictions of the proposed model are compared with experimental results on concrete subjected to cyclic direct tension. Loading regimes of CEN and CSI can be categorized as complete unloading and reloading. Comparison of predicted results with experimental results for envelope curve at various loading strain rates are shown in Fig. 10 and shows a good agreement. Both the unloading and reloading branches are simulated well with experimental results at various strain rates. Fig. 10 has given the comparison of simulated results with experimental results for cyclic with constant strain increment at various strain rates. A series complete unloading and reloading are presented in Figs. 10 and 11. The complete unloading and reloading curves can be reproduce when the point at which unloading begins is given. Comparison of predicted

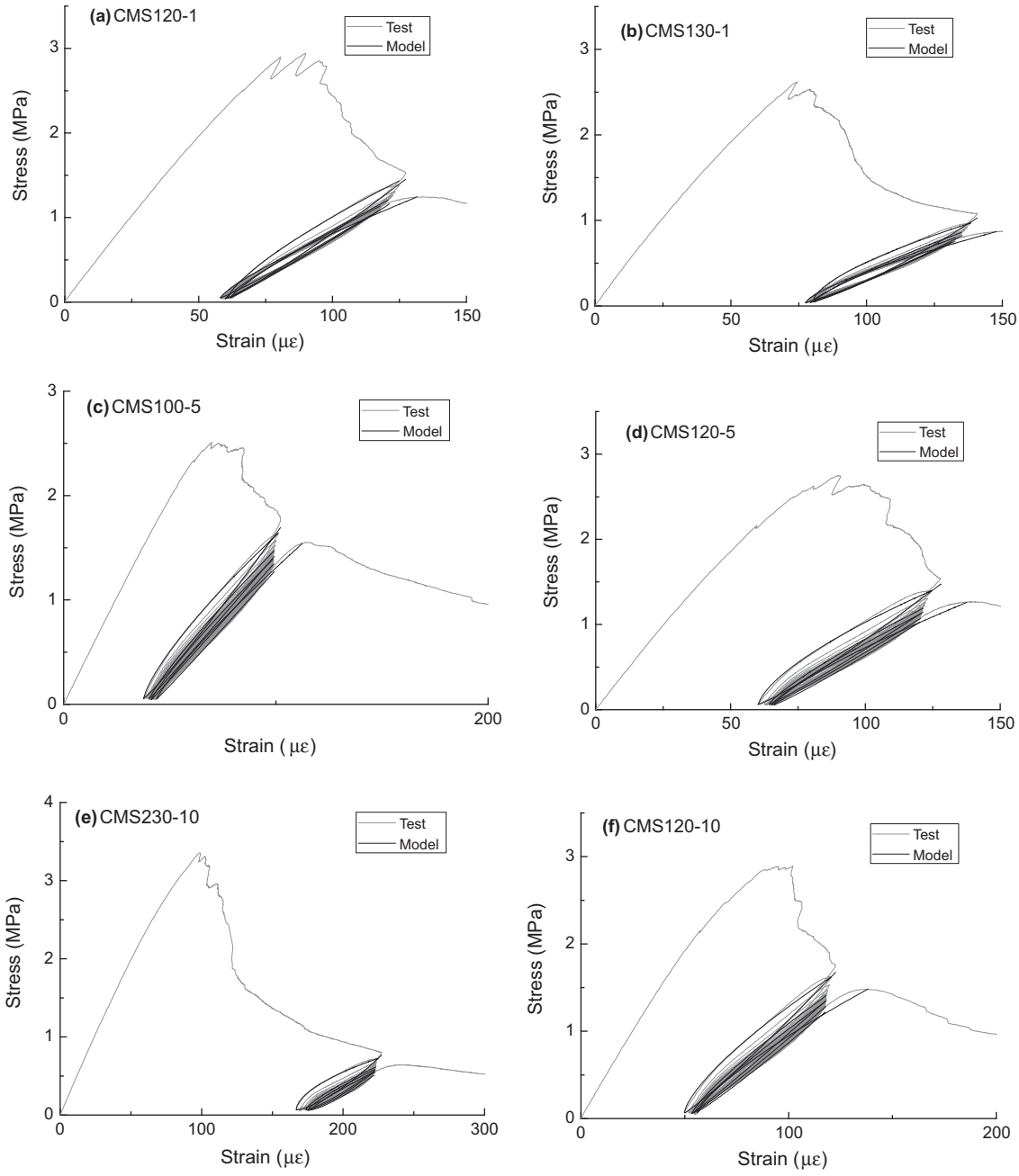

Fig. 12. Comparison of predicted results with experimental tests from cyclic to constant maximum strain at various strain rates.

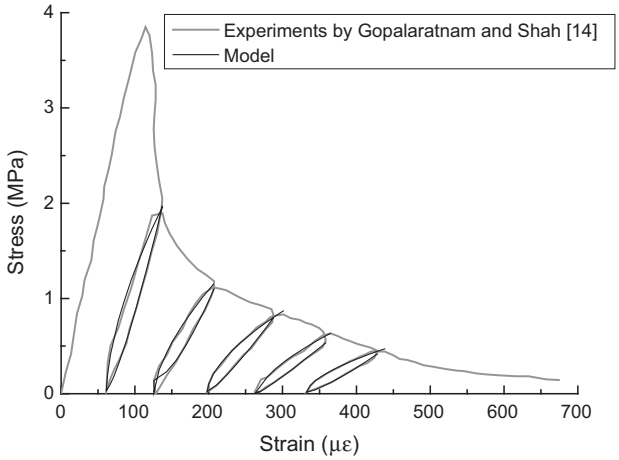

Fig. 13. Comparison of simulated with experimental results from Gopalaratnam and Shah [14].

results with experimental tests for cyclic to constant maximum strain at various strain rates is seen in Fig. 12. In the simulation figure, only the 1st, 5th, 10th, 20th hysteresis cycles are plotted to the experimental results to see clearly. In the case of cyclic to constant maximum strain, incomplete reloading and unloading curves are presented. The location of current reloading or unloading curves due to the previous incomplete unloading or reloading is dependent on the displacement at which the incomplete unloading or reloading terminates. To evaluate the validity of the proposed model in this paper, comparison of simulated and experimental results from other researcher has been made as shown in Fig. 13. It can be seen that the simulated results have good agreement with experimental results.

5. Conclusions

The purposes of this investigation are to study the post-peak cyclic behavior of concrete in tension and the effect of strain rate on the post-peak behavior. A kind of spherical joint is designed to reduce the eccentricity and the load transfers to the specimen by the spherical joints and screws. It demonstrated that the test method can obtain reliable complete monotonic and the post-peak cyclic response of plain concrete subjected to direct tension.

Slightly rate sensitive characteristics can be observed in concrete. The rate of residual strain accumulation increases with the increasing of strain rate. Stress releases even if the maximum strain is kept constant. Damage accumulation rate along the reloading path has been observed independent on the strain rates.

The envelope curve provides the upper bounds for the stress strain curve of concrete under general loading regimes. The concept of uniqueness of envelope curve has also been verified by the experimental results in this paper. Analytical expressions introducing damage index are proposed to describe the entire monotonic behavior, as well the response to cyclic loadings. A good agreement is found between the predicted results by the proposed model and experimental data.

Acknowledgments

This research is based upon work support supported by the National Natural Science Foundation of China (Grant No. 51509078) and Natural Science Foundation of Jiangsu Province (Grant No. BK20150820) and the Fundamental Research Funds for the Central Universities (2016B06014) granted to the first author Xudong Chen.

References

[1] B.P. Sinha, K.H. Gerstle, L.G. Tulin, Stress-strain relations for concrete under cyclic loading, J. Am. Concr. Inst. 61 (2) (1964) 195–211.
[2] J.F. Sima, P. Roca, C. Molins, Cyclic constitutive model for concrete, Eng. Struct. 30 (3) (2008) 695–706.
[3] M. Breccolotti, M.F. Bonfigli, A. D'Alessandro, Constitutive modeling of plain concrete subjected to cyclic uniaxial compressive loading, Constr. Build. Mater. 94 (2015) 172–180.
[4] J. Lee, G.L. Fenves, Plastic-damage model for cyclic loading of concrete structures, J. Eng. Mech. 124 (8) (1998) 892–900.
[5] U. Cicekli, G.Z. Voyiadjis, R.K.A. Al-Rub, A plasticity and anisotropic damage model for plain concrete, Int. J. Plast 23 (10) (2007) 1874–1900.
[6] X. Chen, S. Wu, J. Zhou, Effect of testing method and strain rate on stress-strain behavior of concrete, ASCE J. Mater. Civ. Eng. 25 (2012) 1752–1761.
[7] X. Chen, S. Wu, J. Zhou, Experimental study on dynamic tensile strength of cement mortar using split hopkinson pressure bar technique, ASCE J. Mater. Civ. Eng. 26 (6) (2014).
[8] X. Chen, S. Wu, J. Zhou, Strength values of cementitious materials in bending and tension test methods, ASCE J. Mater. Civ. Eng. 26 (3) (2014) 484–490.
[9] N. Ranaivomanana, M. Stéphane, T. Anaclet, Basic creep of concrete under compression, tension and bending, Constr. Build. Mater. 38 (2013) 173–180.
[10] F. Alhussainy et al., Direct tensile testing of self-compacting concrete, Constr. Build. Mater. 112 (2016) 903–906.
[11] J. Xiao, H. Li, Z. Yang, Fatigue behavior of recycled aggregate concrete under compression and bending cyclic loadings, Constr. Build. Mater. 38 (2013) 681–688.
[12] D.Z. Yankelevsky, H.W. Reinhardt, Model for cyclic compressive behavior of concrete, J. Struct. Eng. 113 (2) (1987) 228–240.
[13] H.W. Reinhardt, H.A.W. Cornelissen, Post-peak cyclic behaviour of concrete in uniaxial tensile and alternating tensile and compressive loading, Cem. Concr. Res. 14 (2) (1984) 263–270.
[14] V.S. Gopalaratnam, S.P. Shah, Softening response of plain concrete in direct tension, J. Am. Concr. Inst. 82 (3) (1985) 310–323.
[15] D. Palermo, F.J. Vecchio, Compression field modeling of reinforced concrete subjected to reversed loading: formulation, ACI Struct. J. 100 (5) (2003) 616–625.
[16] S.J. Foster, P. Marti, Cracked membrane model: finite element implementation, J. Struct. Eng. 129 (9) (2003) 1155–1163.
[17] M. Mansour, T.T.C. Hsu, Behavior of reinforced concrete elements under cyclic shear. II: theoretical model, J. Struct. Eng. 131 (1) (2005) 54–65.
[18] Z. Tian, J. Bu, C. Bian, Effect of strain rate and saturation on uniaxial dynamic compressive behaviours of mortar, Int. J. Pavement Eng. (2015) 1–10 (ahead-of-print).
[19] ASTM C 33, Standard Specification for Concrete Aggregates, American Society for Testing and Materials, West Conshohocken, PA, 2004.
[20] A. Maher, D. Darwin, Mortar constituent of concrete in compression, ACI J. Proc. 79 (2) (1982) 100–109.
[21] B.Y. Bahn, C.T.T. Hsu, Stress-strain behavior of concrete under cyclic loading, ACI Mater. J. 95 (2) (1998) 178–193.
[22] D.E. Otter, A.E. Naaman, Properties of steel fiber reinforced concrete under cyclic load, ACI Mater. J. 85 (4) (1998) 254–261.
[23] F.J. Vecchio, M.P. Collins, The modified compression-field theory for reinforced concrete elements subjected to shear, J. Am. Concr. Inst. 83 (2) (1986) 219–231.
[24] P.E. Petersson, Crack growth and development of fracture zones in plain concrete and similar materials, Division, Institute (doctoral dissertation), 1981.